Human lateral Frontal Pole contributes to control over social-emotional behaviour

Running title: FPl in social-emotional control

Bob Bramson[1], Davide Folloni[3,4], Lennart Verhagen[3,4], Bart Hartogsveld[5], Rogier B. Mars[1,4], Ivan Toni[1,*] and Karin Roelofs[1,2,*]

[1]Donders Institute for Brain, Cognition and Behaviour, Centre for Cognitive Neuroimaging, Radboud University Nijmegen, 6525 EN Nijmegen, The Netherlands

[2]Behavioural Science Institute (BSI), Radboud University Nijmegen, 6525 HR Nijmegen, The Netherlands

[3]Wellcome Centre for Integrative Neuroimaging (WIN), Department of Experimental Psychology, University of Oxford, Oxford, OX1 3SR, United Kingdom

[4]Wellcome Centre for Integrative Neuroimaging (WIN), Centre for Functional MRI of the Brain (FMRIB), Nuffield Department of Clinical Neurosciences, John Radcliffe Hospital, University of Oxford, Oxford, OX3 9DU, United Kingdom

[5]Faculty of Psychology, Maastricht University, 6229 ER Maastricht, The Netherlands

* These authors contributed equally

Correspondence:
Bob Bramson
Donders Centre for Cognitive Neuroimaging
Radboud University Nijmegen
Trigon Building
Kapittelweg 29
6525 EN Nijmegen
The Netherlands
Phone: +31(0)24 3622400
E-mail: b.bramson@donders.ru.nl

Abstract

Emotion regulation is essential for human social interactions. Recent work has exposed its cognitive complexity, as well as its unexpected reliance on portions of the anterior prefrontal cortex (aPFC) also involved in relational reasoning, rather than on dorsolateral and medial prefrontal areas involved in several forms of cognitive control. This study anatomically qualifies the contribution of aPFC territories to the regulation of social-emotional actions, relating emotional regulation to other cognitive processes that have been associated with the aPFC, and explores a possible structural pathway through which emotional regulation might be implemented.

We provide converging evidence from task-based fMRI, diffusion-weighted imaging, and resting-state connectivity fingerprints for a novel neural element in emotion regulation. Task-based fMRI differentiated, within the same participants, aPFC territories involved in social-emotional regulation from territories known to support relational processing. Connectivity fingerprints, based on diffusion-weighted imaging and resting-state connectivity, localized those task-defined frontal regions to an anatomically-defined portion of the aPFC, the lateral frontal pole (FPl). Probabilistic tractography indicated that a fifth of inter-individual variation in social-emotional regulation abilities is accounted by the strength of structural connectivity between FPl and amygdala. These findings provide novel neuroanatomical evidence for incorporating FPl in models of social-emotional regulation.

Keywords: social-emotional regulation, amygdalofugal connectivity, prefrontal control, approach-avoidance, lateral frontal pole

Introduction

Being able to control social-emotional behaviour is paramount for successful participation in society (Hare 2017). However, regulating social-emotional actions is cognitively complex. It requires the ability to assess the effectiveness of on-going behaviour and compare this with alternative action strategies, whilst maintaining a representation of complex social relations that might be influenced by the selected behaviour. By way of example: police officers facing a pointed gun from a terrorist need to overcome their automatic action tendency to avoid the threat, while selecting a course of action from several alternative behavioural possibilities, without ignoring the potential consequences of those actions on surrounding people. Recent converging evidence indicates that this type of social-emotional regulation is computed in the most rostral part of the anterior prefrontal cortex (aPFC) (Volman et al. 2011, 2013; Tyborowska et al. 2016; Koch et al. 2018). The current study anatomically qualifies the contribution of aPFC regions to the regulation of social-emotional action, and explores a possible structural pathway through which this regulation might be implemented.

The aPFC has been involved in a disparate range of cognitive tasks [e.g. relational reasoning (Vendetti and Bunge 2014; Hartogsveld et al. 2017), counterfactual choice (Boorman et al. 2009a; Mansouri et al. 2017), exploration behaviour (Daw et al. 2006; Zajkowski et al. 2017)]. Yet, to date, emotional regulation has not been considered part of the cognitive fingerprint of this region (Koch et al. 2018). Models of emotion regulation have largely focused on dorsolateral and medial prefrontal areas (Etkin et al. 2015; Morawetz et al. 2017; Langner et al. 2018). At first glance, the focus of the emotion control literature on medial prefrontal cortex (mPFC) is justified by the strong structural and functional connectivity between mPFC and areas involved in emotional and social processing, such as the amygdala (Ghashghaei and Barbas 2002; Petrides and Pandya 2007; Neubert et al. 2014; Motzkin et al. 2015; Tillman et al. 2018). In contrast, structural connections to the amygdala are scarce for anterior prefrontal areas (Ghashghaei et al. 2007). However, recent studies have shown that amygdala is connected to the aPFC via the rostral projections of the ventral amygdalofugal pathway

(Krüger et al. 2015; Kamali et al. 2016). In fact, there is evidence that this tract might extend to the lateral frontal pole (FPl;Folloni et al. 2019)), a portion of the human aPFC that does not have a homological counterpart in macaque brains (Ramnani and Owen 2004; Semendeferi et al. 2010; Neubert et al. 2014). These anatomical observations, together with converging functional evidence on aPFC involvement in the regulation of emotional strategies and actions (Koch et al. 2018), raise the possibility that human social-emotional control is coordinated by the FPl.

In this study, we combine evidence from task based fMRI, diffusion-weighted imaging, and resting-state connectivity fingerprints to define which portion of aPFC supports social-emotional control, and how that function anatomically relates to other cognitive processes that have been associated with the aPFC. First, we characterize the functional specificity of aPFC contributions to social-emotional regulation. We contrast the cortical territories supporting two functions previously associated with the aPFC region, indexed through a social-emotional approach-avoidance (AA) task and a relational reasoning (RR) task (Vendetti and Bunge 2014). Second, we anatomically localize the aPFC territories activated by the approaach-avoidance and relational-reasoning tasks. We match their structural and functional connectivity fingerprints to the fingerprints extracted from known areas of the aPFC (Neubert et al. 2014). Third, we assess the evidence for a possible structural pathway through which the portion of the aPFC activated by the AA task might support social-emotional regulation, namely through connections with the amygdala (Folloni et al. 2019)

Methods

Participants

Forty male students from the Radboud University Nijmegen participated in this study after giving informed consent. All participants took part in the social AA task, diffusion weighted imaging, and resting-state scans. A subsample (n = 19) participated in the higher-order relational-reasoning

task. The total sample had a mean age of 23.5 years (sd: 2.8, range 18-33 years), the relational-reasoning task sub-sample had a mean age of 24.8 years (sd: 4.2, range 18-33). None of the participants reported history of mental illness or use of psychoactive/corticosteroid medication. All had normal or corrected to normal vision, and were screened for counter indications for magnetic resonance imaging (MRI). The study was approved by the local ethics committee (CMO:2014/288).

Materials and apparatus

Images were acquired using a 3 T MAGNETROM Prisma MRI scanner (Siemens AG, Healthcare Sector, Erlangen, Germany) using a 32 channel headcoil for functional and DWI images and a 20 channel headcoil for structural T1 images. Stimuli were presented using an EIKI LC- XL100 beamer with a resolution of 1024 x 768 and a refresh rate of 60 Hz, and were projected onto a screen behind the scanner bore. Participants were able to see the screen via a mirror.

The approach-avoidance (AA) task consisted of 16 blocks of 12 trials each, in which participants had to approach or avoid equiluminant happy or angry faces presented in the centre of the screen. Faces were presented for 100 ms and preceded by a 500 ms fixation cross in the centre of the screen. After the presentation of the face, participants had 2000 ms to respond using a joystick. Each trial was followed by an intertrial interval of 2 – 4 seconds. Task instructions for congruent (move the joystick towards you/away from you for happy/angry faces), and incongruent blocks (move the joystick towards you/away from you for angry/happy faces), were presented before each block and switched between blocks. Subjects responded using a customized fiber optic response joystick, which was fixed to only move in the saggital plane. Affect-incongruent trials have consistently been shown to activate the aPFC (Roelofs et al. 2008; Volman et al. 2011; Tyborowska et al. 2016).

The relational reasoning tasks consisted of 80 trials in which participants were presented a screen containing two pairs of stimuli. Participants had to make judgments about the relation between stimuli within each pair (lower-order relation trials) or on the relation between the two

within-pair relations (higher-order relation trials). There were two versions of the task; social and non-social. Images in the non-social task differed in texture and shape. Images in the social task consisted of faces that differed on the dimensions age and ethnicity. These conditions are both described in detail in Hartogsveld et al. (2017) and depicted in figure 4A. This paradigm has been shown to elicit activity in the rostrolateral prefrontal cortex (Vendetti and Bunge 2014) and a recent study (Hartogsveld et al. 2017) has shown that this area is the same as the FPl identified by Neubert et al. (2014).

Procedure

Data were acquired on two different days; one day consisted of the AA task, resting-state and T1 structural scan. The other day consisted of the relational reasoning task and DWI. Order of days was randomized over participants. Before and after each scan day we took saliva measurements to possibly control for testosterone and cortisol for other research purposes. On the second day each participant filled out the State Trait Anxiety Inventory to control for effects of trait anxiety.

Functional scans

The field of view of the scans acquired in the two MR-sessions was aligned to a built-in brain-atlas using an auto-align head scout sequence. During resting state and task fMRI sessions we acquired BOLD-sensitive images using a multiband sequence with TR = 735 ms/TE = 39ms, 64 slices, flip angle of 52°, multiband acceleration factor of 8, slice orientation T > C, voxel size = 2.4 x 2.4 x 2.4 mm, phase encoding direction A >> P. The resting state session lasted 8.5 minutes (700 images). Each sequence was followed by a field map image; flip angle = 60°, TR = 614, TE = 4.92.

Structural scan

High-resolution anatomical images were acquired with a single-shot MPRAGE sequence with an acceleration factor of 2 (GRAPPA method), a TR of 2400 ms, TE 2.13 ms. Effective voxel size was 1 x 1 x 1 mm with 176 sagittal slices, distance factor 50%, flip angle 8°, orientation A ≫ P, FoV 256 mm.

DW imaging

Diffusion-weighted images were acquired using echo-planar imaging with an acceleration factor of 2 (GRAPPA method). We acquired 65 2 mm-thick axial slices, with a voxel size of 2 x 2 x 2 mm, phase encoding direction A >> P, FoV 220 mm. In addition, we acquired 10 volumes without diffusion weighting (b = 0 s/mm^2), 30 isotropically distributed directions using a b-value of 750 s/mm^2, and 60 isotropically distributed directions a b-value of 3000 s/mm^2. We also acquired a volume without diffusion weighting with reverse phase encoding (P >> A).

Behavioural analyses

Behavioural analyses of AA task performance contrasted incongruent to congruent trials, comparing reaction times and percentage correct between conditions. Differences between conditions were assessed using paired-sample t-tests for the approach-avoidance task, and repeated measures ANOVAs for the relational reasoning task.

Analyses - functional images

All processing of the AA and resting state images was done using MELODIC 3.00 as implemented in FSL 5.0.10 (https://fsl.fmrib.ox.ac.uk). Images were motion corrected using MCFLIRT (Jenkinson et al. 2002), and distortions in the magnetic field were corrected using fieldmap correction in FUGUE. Functional images were rigid-body registered to the brain extracted structural image using FLIRT. Registration to MNI 2mm standard space was done using the nonlinear registration tool FNIRT. Images were spatially smoothed using a Gaussian 5 mm kernel and low passed filtered with a cut-off at 100 s. Independent component analysis was run (Beckmann and Smith 2004), after which the first 10 components were manually inspected to remove sources of noise (Griffanti et al. 2017). Preprocessing for the higher-order relational reasoning task consisted of a similar procedure, which is described in detail in Hartogsveld et al. (2017).

First and second level analyses were done in FEAT 6.00 implemented in FSL 5.0.10. We set up separate general linear models for each task. The first-level AA model consisted of four task regressors: Approach angry, approach happy, avoid angry and avoid happy; six motion regressors and their temporal derivatives; and two regressors modelling fluctuations in signal in white matter and cerebrospinal fluid. Approach happy and avoid angry (congruent conditions) were then contrasted with approach angry and avoid happy (incongruent conditions). This contrast was taken as input for each subject in the second level analysis. Second level analysis was performed using FMRIB's Local Analysis of Mixed Effects (FLAME 1) with outlier de-weighting. We used a cluster forming threshold of $Z > 2.3$, a value that has been shown to effectively control for Family Wise Error rate, possibly related to the fact that FLAME estimates and takes into account within subject variance (Eklund et al. 2015). Locations with above threshold activity were localized using masks for the prefrontal cortex (Sallet et al. 2013; Neubert et al. 2014), parietal cortex (Mars et al. 2011) and whole brain cortical and subcortical atlases (Harvard-Oxford atlas). For the relational reasoning task we contrasted lower-order and higher-order conditions, full methods used for this task are described in (Hartogsveld et al. 2017).

To assess psychophysiological interactions (PPI) during the AA task we ran a second analysis using FEAT with regressors representing the task effects of interest (incongruent-congruent), the regressor incongruent + congruent, a regressor describing the first eigenvariate time series of activation of the seed region: Bilateral amygdalae taken from the AAL atlas (Tzourio-Mazoyer et al. 2002), and a regressor describing the interaction between the seed region activity and task effects. Strength of amygdalofugal-FPl connections as estimated from tractography of dw-MRI (see below) was added as a covariate in the second level analysis.

For the conjunction analysis between activation in the AA and the higher-order reasoning task we overlaid the cluster thresholded contrast maps from both tasks.

Analyses – functional connectivity fingerprints of FPl based on resting-state fMRI

For the resting state fMRI analysis we defined regions-of-interest for each of the three areas in aPFC (FPl, FPm, and 46), as identified by Neubert et al. (2014). These masks were thresholded to contain only the 25% of voxels that were most likely to be part of each area (Mars et al. 2016; Hartogsveld et al. 2017). The masks were warped to each individual anatomical space, after which we extracted the first eigenvariate time series from each area. These time series were correlated with whole brain resting state activity, the results of which were transformed to z-values using Fishers z-transform and normalized. Resulting correlation maps were transformed back to MNI space after which we extracted the connectivity from each prefrontal region with five downstream regions: Posterior Cingulate Cortex (PCC) [10 -52 24], Intraparietal lobule (IPL) [48 -46 48], temporal pole (TP) [34 12 -36], ventromedial prefrontal cortex (vmPFC) [8 44 -14] and dorsolateral prefrontal cortex (dlPFC) [46 20 40] (see Mars et al. 2016; Hartogsveld et al. 2017), for each hemisphere separately. This procedure gives a "connectivity fingerprint" of each region, describing functional (and structural for DWI analyses) connections with other brain areas, and rests on the premise that each regions' unique functional repertoire is determined by its connections with other regions (Passingham et al. 2002; Mars et al. 2018). We followed the same procedure for the two regions found in the aPFC during the AA task: 5 mm sphere around MNI [24 50 -4] and MNI [-24 52 4].

For the statistical analysis we computed Manhattan distance between the connectivity profiles of the AA regions and the connectivity profiles of the three prefrontal masks, separately for each hemisphere. We compared these distance measures to a distribution of randomized distances that we created by permuting the region labels 10000 times, each time randomly swapping the target region labels (FPl; FPm; area 46) within participants and computing the Manhattan distance with the AA fingerprint. The result of this approach shows whether the connectivity profile of the aPFC regions differs from the connectivity profile of the region active during the AA task (Mars et al. 2016).

Analyses – structural connectivity fingerprints of FPL based on diffusion-weighted MRI

224 All analyses of diffusion data were performed in FSL FDT 3.0 (https://fsl.fmrib.ox.ac.uk). We
225 used TOPUP to estimate susceptibility artifacts using additional b = 0 volumes with reverse phase
226 coding direction (Andersson et al. 2003). Next, we used EDDY (using the fieldmap estimated by
227 TOPUP) to correct for distortions caused by eddy currents and subject movement (Andersson and
228 Sotiropoulos 2016). We used BedpostX to fit a crossing fiber model using default settings (Behrens et
229 al. 2007).

230 Seed regions were defined for five major tracts (see Hartogsveld et al., 2017) by creating 5
231 mm spheres in the Cingulum Bundle (CB) MNI: [8 -2 36], Superior Longitudinal Fasciculus 1 (SLF1),
232 MNI: [16 -2 54], SLF 2, MNI: [30 -2 38], SLF 3, MNI: [44 -2 26] and Uncinate Fasciculus, MNI: [32 -2 -
233 10] and then warped to individual subject space. The procedure for Amygdalofugal connectivity is
234 described below. For the comparisons in the left hemisphere the same coordinates were used with
235 the x-axis coordinate inverted. ProbtrackX was run with default settings using these masks as seed,
236 separately for each hemisphere using an exclusion mask at x = 0. The results from probtrackX were
237 warped to MNI 1 mm space, log transformed, and normalized to the highest probability per tract to
238 allow a direct comparison between tracts with all values ranging between 0 and 1. We computed
239 connectivity profiles of FPl, FPm and area 46 by counting the number of times each tract ended in
240 these regions. These connectivity profiles were compared to the connectivity profile of the region in
241 the aPFC resulting from the AA task contrast (5 mm sphere at MNI: [24 50 -4] for right and MNI: [-24
242 52 4] for left). We computed Manhattan distance between the connectivity profiles of the AA task
243 and the three prefrontal masks and permuted this 10,000 times, each time randomly swapping the
244 target region labels (FPl; FPm; area 46) within participants.

245 *Analyses - Amygdalofugal connectivity*

246 Connections between amygdala and aPFC were reconstructed using probtrackX. For this we
247 used the procedure and masks provided by Folloni et al., (2019). We seeded these connections in the
248 white matter punctuating the extended amygdala and substantia innominata: MNI: [-7 3 -9] and an

249 all-coronal waypoint mask at y = 22. We used tractography masks to ensure the estimated seedlines
250 extended only rostrally, at least up to the y = 25 coronal plane, and excluded CSF and between-
251 hemisphere connections. Connection strength was normalized and log transformed within each
252 participant. Next we extracted the total amount of times the tractography entered the FPl, FPm and
253 area 46 regions-of-interest separately. These values were correlated with congruency effects on
254 reaction time and percentage correct using Spearman's correlation coefficient.

255 To exclude that the Amygdalofugal-FPl connections are influenced by (much stronger)
256 projections of the Uncinate Fasciculus (UF), we reconstructed UF connectivity with FPl and correlated
257 this with the behavioural congruency. To isolate the UF we placed a seed in the white matter rostro-
258 laterally to the amygdala (MNI: [35 2 -22]), a coronal waypoint mask at y = 22 and exclusion masks in
259 the CSF and between hemispheres. We also used partial correlation to regress out possible
260 correlations influences of UF and state anxiety (STAI-Y2) in the amygdalofugal-behavioural
261 correlations.

262 **Results**

263 The study had two main goals: i) localize aPFC responses evoked during control over social-
264 emotional action tendencies in relation to an established anatomical parcellation of the aPFC, and in
265 relation to aPFC responses evoked during relational reasoning; and ii) provide evidence for the
266 functional relevance of amygdala-aPFC connectivity in implementing control over emotional-actions.
267 We implemented a-priori determined analyses addressing these two goals, correcting the statistical
268 inferences for multiple comparisons, either through cluster correction (fMRI task contrasts), or
269 Bonferroni-correction (anatomical localization and tract-behavioral correlations). Furthermore, we
270 implemented a number of follow-up exploratory analyses, prioritizing sensitivity over specificity, thus
271 avoiding corrections for multiple comparisons. The exploratory nature of these analyses is marked in
272 the text.

273 *AA-task - Behavioral costs of controlling social-emotional behavior*

Reaction times were longer for incongruent (M = 673 ms, SD = 103) than for congruent movements (M = 626 ms, SD = 128), $t(39) = 5.12$, $p < .001$ with an effect size of $d = .4$, CI [.22 , 1.03], calculated as (M1-M2) / sd_{pooled}]. Participants also made more errors during incongruent (M = 94.3 % correct, SD = 4.43) than congruent blocks (M = 97.1 % correct, SD = 2.96), $t(39) = 5.21$, $p < .001$; effect size $d = .7$, CI [.27 , 1.2]. Behavioral effects are shown in figure 1B. These effects illustrate the behavioral cost of applying cognitive control over prepotent social-emotional action tendencies.

AA-task - Controlling social-emotional actions elicits frontal and parietal activation

Building on previous evidence (Volman et al. 2011; Tyborowska et al. 2016), we expected that control over social emotional action tendencies increases aPFC activity. This study tests whether this activity is localized to the lateral Frontal Pole. We found clusters of increased activity over frontal areas during incongruent as compared to congruent trials, whole-brain cluster-level corrected for multiple comparisons (cluster-forming threshold of $Z > 2.3$ with corrected cluster threshold of $p < .05$). Overlaying the frontal activity profiles on the mask created by Neubert et al. (2014) confirmed activity in FPl, figure 1C. In addition we observed clusters of increased activity in bilateral intraparietal lobule, an area strongly connected to the aPFC (Mars et al. 2011); bilateral Insula/Inferior Frontal Gyrus [34 26 -6]; Bilateral area 8A [40 6 42]; bilateral area 46 [30 50 16]; and bilateral cerebellum [16 -78 -30].

The estimated BOLD signal indexing control over emotional action tendencies (incongruent vs congruent trials) extracted from FPl correlated positively with the behavioral index of emotional control (reaction time differences between incongruent and congruent trials): $r(38) = .33$, $p = .037$, figure 1D. This effect corroborates our earlier findings of a positive relationship between individual differences in reaction time effects and recruitment of aPFC/FPl activation (Roelofs et al. 2009; Bramson et al., 2018). Exploratory analyses correlating BOLD congruency with behavioral congruency gave a trend correlation for area 46; $r(38) = .31$, $p = .05$ and no correlation for FPm; $r(38) = .07$, $p =$

298 .63, suggesting anatomical specificity in the involvement of FPl in controlling social-emotional

299 behavior.

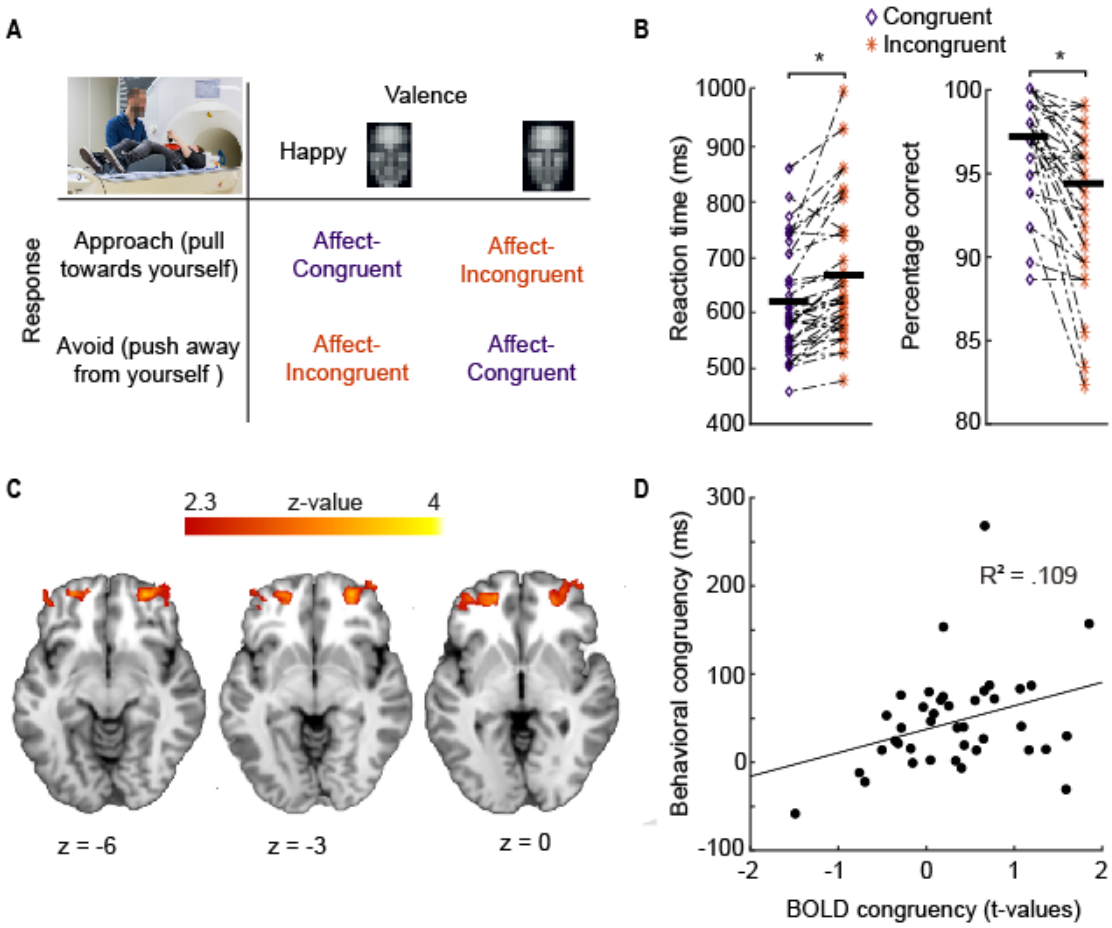

300

301 ***Figure 1: Effects of cognitive control over social-emotional action tendencies.***

302 *A) Schematic representation of the AA task used to measure control over social-emotional action*

303 *tendencies. The incongruent condition requires control to override the automatic tendencies to*

304 *approach happy- and avoid angry faces. B) Behavioural effects on AA task; participants show longer*

305 *reaction times and more errors during the incongruent condition, illustrating the cost of exerting*

306 *control. C) Main task effects for incongruent > congruent, masked to show above threshold (cluster*

307 *level p < .001) activation in the anterior Prefrontal Cortex. (Frontal Pole mask; Harvard-oxford atlas)*

308 *D) Correlation between reaction time congruency and BOLD congruency effects extracted from the*

309 *lateral Frontal Pole across participants.*

Relation between AA-related activity and functional fingerprints of FPl (Resting-state connectivity)

To assess whether the aPFC activity evoked during social-emotional control falls within FPl (Neubert et al. 2014), we compared resting-state connectivity profiles of area 46, FPl and FPm with the connectivity profile of the aPFC clusters showing a congruency effect (MNI: [24 50 -4] and [-24 52 -4]). We tested whether the connectivity fingerprints of the three prefrontal areas differed from the connectivity profile of the AA-related clusters.

Resting-state fingerprints of area 46 and FPl showed relatively similar connectivity profiles, both being strongly correlated with the Intraparietal lobule (IPL) and dorsolateral prefontal cortex (dlPFC), but slightly stronger connectivity of FPl to the Posterior Cingulate Cortex (PCC). Functional connectivity of FPm differed quite strongly from both area 46 and FPl, with strongest connectivity with ventromedial prefrontal areas (vmPFC), PCC and temporal Pole (TP), figure 2A;C. These results corroborate earlier reports on resting-state connectivity fingerprints for these areas (Neubert et al. 2014; Mars et al. 2016; Hartogsveld et al. 2017).

Comparing connectivity profiles between the three areas in aPFC with the connectivity profile extracted from the AA-related region showed that its fingerprint differed significantly from that of area 46, (left hemisphere: $p < .001$; right-hemisphere: $p < .001$), and from that of area FPm (right hemisphere: $p < .001$; left-hemisphere: $p < .001$), but not from the connectivity fingerprint of area FPl (left-hemisphere: $p = .87$, right-hemisphere: $p = .075$), figure 2E. This result provides evidence that control of social emotional action tendencies involves the lateral Frontal Pole.

Relation between AA-related activity and structural fingerprints of FPl (DWI connectivity)

In addition to resting-state connectivity, we created connectivity profiles based on white matter tractography. We placed seeds in five large white matter tracts (figure 2B); performed probabilistic tractography to the rest of the hemisphere; and counted how often each tract ended in

333 each of the three regions in aPFC (figure 2B). We used a similar procedure for amygdalofugal (AmF)
334 connectivity (see methods).

335 Comparing connectivity profiles of the aPFC regions to these five major white matter tracts
336 and AmF connectivity showed relatively strong connectivity between area 46 and the three superior
337 longitudinal fasciculi (SLF1, SLF2 and SLF3; figure 2D). FPm is most strongly connected to the
338 Cingulate Bundle, Uncinate Fasciculus and Amygdalofugal pathways. FPl is less strongly connected to
339 the tracts leading outside the frontal cortex, and more strongly connected to the Uncinate Fasciculus,
340 which leads to the temporal pole (among other regions). The AA-related regions are also more
341 strongly connected to the Uncinate Fasciculus. These results are shown in figure 2D and match
342 earlier reports on connectivity of aPFC regions (Neubert et al. 2014; Mars et al. 2016; Hartogsveld et
343 al. 2017).

344 Comparing connectivity profiles between the three areas in aPFC with the connectivity
345 profile extracted from the AA region showed that the fingerprint of the AA region differed
346 significantly from that of area 46, (left hemisphere: $p < .001$; right-hemisphere: $p < .001$), and from
347 that of area FPm (right hemisphere: $p < .001$; left-hemisphere: $p < .001$), but not from the
348 connectivity fingerprint of area FPl (left-hemisphere: $p = .98$, right-hemisphere: $p = 1$), figure 2F. This
349 result corroborates the resting state results, providing additional evidence that the FPl is one of the
350 regions involved in controlling social emotional action tendencies.

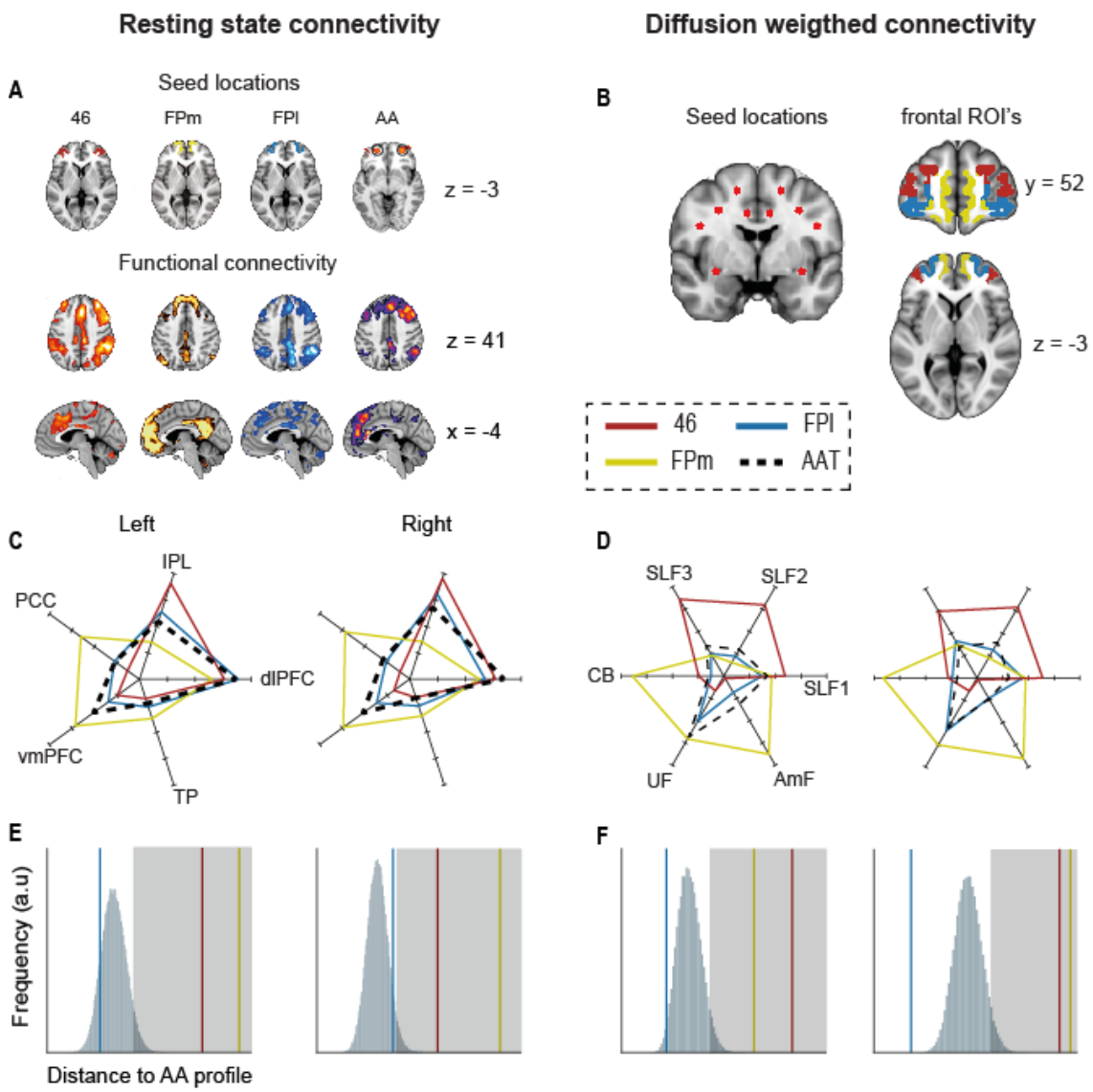

Figure 2: AA task effects are localized within the connectivity-defined lateral Frontal Pole.

A) Seed regions and whole brain resting-state connectivity for area 46, FPm, FPl, and for the cluster showing AA task-effects. B) Seed locations for tractography in five large white matter tracts (AmF seed not shown) and masks for the regions FPl, FPm and area 46. C) Resting state connectivity fingerprints of the aPFC and AA regions, separated for left and right ROI's. Region labels: Posterior Cingulate Cortex (PCC), ventromedial prefrontal cortex (vmPFC), Intraparietal Lobule (IPL), dorsolateral Prefrontal Cortex (dlPFC), Temporal Pole (TP). D) Connectivity fingerprints for tractography of aPFC and the AA regions, separated for left and right ROI's. Tract abbreviations:

Superior Longitudinal Fasciculus (SLF1, SLF2, SLF3); Uncinate Fasciculus (UF); Cingulum Bundle (CB); Amygdalofugal (AmF). E) and F) Permutation results, where the Manhattan distance between each region's connectivity fingerprint is compared to the fingerprint of the AA region. Area 46 and FPm differ significantly from the AA region in both structural and functional connectivity, whereas the FPl does not. Grey area exceeds threshold of .05: exceeding this threshold means that the difference between the connectivity profile of that region is different from that of the AA region.

FPl-amygdalofugal connectivity partly explains performance on the AA task.

To identify an anatomical pathway through which the FPl could support social-emotional behavior, we tested whether inter-subject variability in the strength of FPl structural connectivity mediated by the amygdalofugal connections predicts successful performance on the AA task. On average, the FPm is more strongly connected to amygdalofugal pathways than the FPl and area 46 (Figure 3A), in line with earlier studies showing both functionally and anatomically stronger connections between limbic areas and medial prefrontal regions (Ghashghaei and Barbas 2002; Neubert et al. 2014; Folloni et al. 2019). However, individual variability in the connectivity of FPl and FPm confirms that the former region is more strongly involved in social-emotional control than the latter. There was a significant correlation between tract strength and AA congruency effect on percentage correct $r(38)$ .44 =, p = .0044 for the FPl connections but not for FPm, $r(38)$ = .24, p = .13 and area 46, $r(38)$ = .3, p = .062, figure 3B. However, these correlations did not differ from one another, both comparisons p > .3. The direction of the FPl-behavioral correlation indicated that stronger connectivity was related to relatively worse performance when having to exert control. There were no significant correlations between tract strength and congruency effect on reaction time; all p > .09. The congruency-FPl correlation for percentage correct survives Bonferroni-correction for multiple comparisons over the eight correlations computed between behavioral congruency and amygdalofugal-FPl connectivity; and the two control correlations described below.

To facilitate data interpretation, we conducted 2 additional exploratory control analyses. First, to exclude that the correlation between amygdalofugal-FPl connectivity and AA performance could be better explained by connections between amygdala and FPl through the Uncinate Fasciculus (UF; Petrides and Pandya 2007) or trait anxiety (Kim and Whalen 2009), we correlated UF-FPl connectivity with AA performance, and amygdalofugal-FPl connectivity with scores on the State anxiety inventory (STAI). None of these analyses yielded significant correlations, all $p > .58$. Nor did the correlation between amygdalofugal-FPl connections and behavioral congruency change when controlling for state anxiety or UF-FPl connectivity.

Second, to explore whether FPl-amygdalofugal connectivity would also influence functional connectivity between these two areas, we performed a Psychophysiological Interaction (PPI) analysis with bilateral amygdalae as seed region and the strength of the connection with FPl as covariate. This analysis showed a negative correlation between tract strength and amygdala-FPl functional connectivity during the task, when using a small volume correction over bilateral FPl; $p = .019$ (FWE cluster corrected; cluster location MNI [-32 50 6], cluster size: 20 voxels), meaning that with increased tract strength there is more negative connectivity between the FPl and amygdala, which might be interpreted as increased regulation of amygdala by the FPl (Volman et al. 2013). However, the peak voxel level analysis did not show a significant effect: $p = .12$, indicating that these connectivity results should be interpreted with caution.

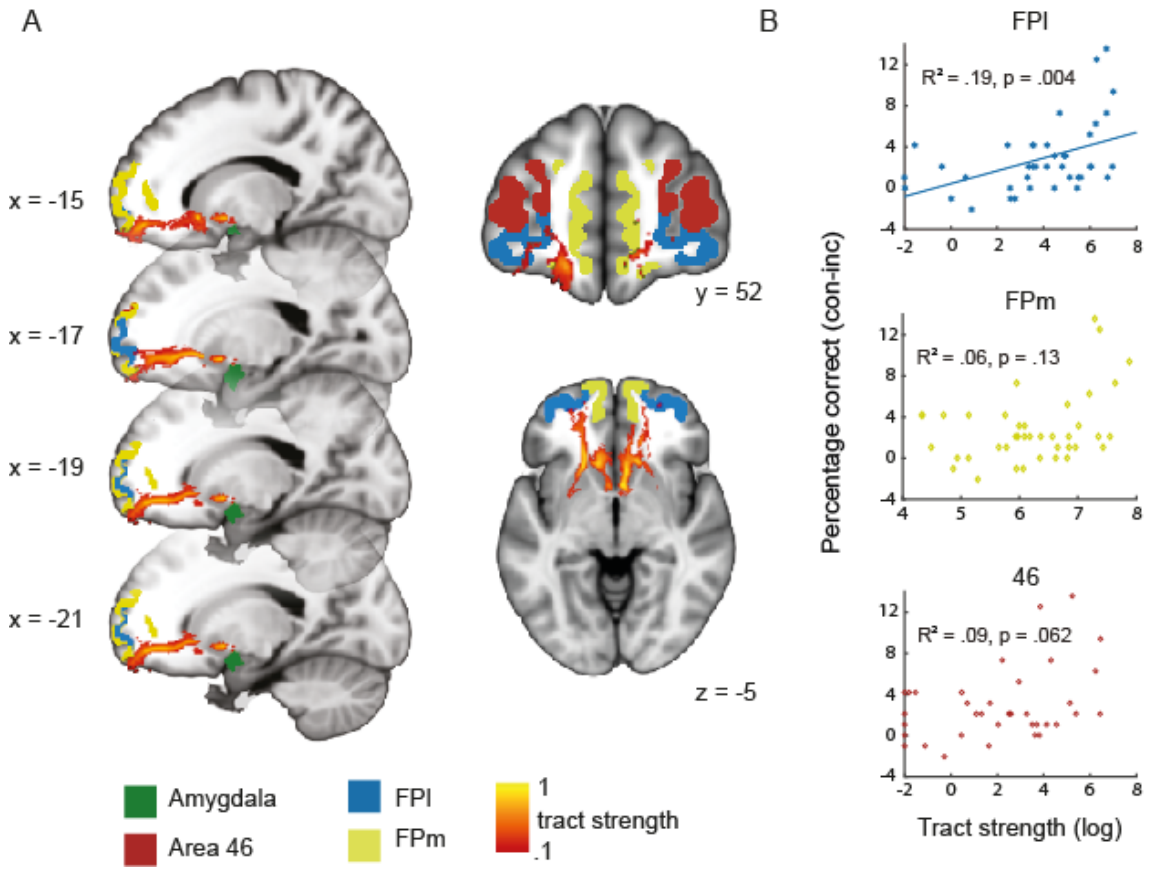

Figure 3: Amygdalofugal connections with FPl correlate with AA task performance. *A) Illustration of the reconstructed tract that leads from the Amygdala to the anterior Prefrontal cortex. This tract shows strongest connectivity with medial prefrontal areas, as can be expected given earlier studies. B) The number of times the tract ends in FPl correlates with behavioural congruency in error rates on the AA task, r = -.44, p = .0044, suggesting that the amygdalofugal pathway is involved in mediating FPl-amygdala functional interactions during social-emotional control.*

RR task - Behavioral costs of higher order relational reasoning

Reaction times were longer for higher-order than low-order relation trials, both for non-social (M =1971 ms; SD = 517 for higher order; M = 2386 ms; SD = 650 for low-order) and social conditions (M = 3673 ms; SD = 887 for higher order; M = 3123 ms; SD = 752 for lower order); repeated measures ANOVA on trial-dimension: $F(1,18) = 103.6$, $p < .001$. Participants also made more

mistakes during the higher-order trials as compared to the low-order both for nonsocial (% correct: M = 81% SD = 16.4 for high-order; M = 93 %; SD = 9.5 for low-order) and social conditions (% correct: M = 66% SD = 7.2 for high-order; M = 71% SD = 8.5 for low-order); repeated measures ANOVA on trial-dimension: $F(1,18) = 63.3$ $p < .001$. These results illustrate the computational cost of higher-order relational reasoning.

Distinct FPl sub-structures in social-emotional control and higher-order relational reasoning

As reported in Hartogsveld et al., (2017), neural effects of the relational reasoning task have previously been localized to the FPl using the same connectivity fingerprinting approach as used in this study. However, overlaying the effects of the AA and the two versions of the relational reasoning task showed only minor overlap in the FPl (figure 4B; C), with more rostro-lateral activity elicited by relation reasoning as compared to the activity elicited in social-emotional control. There is some overlap in area 46, which might be interpreted as reflecting the dependence of task performance on the correct maintenance of response rules.

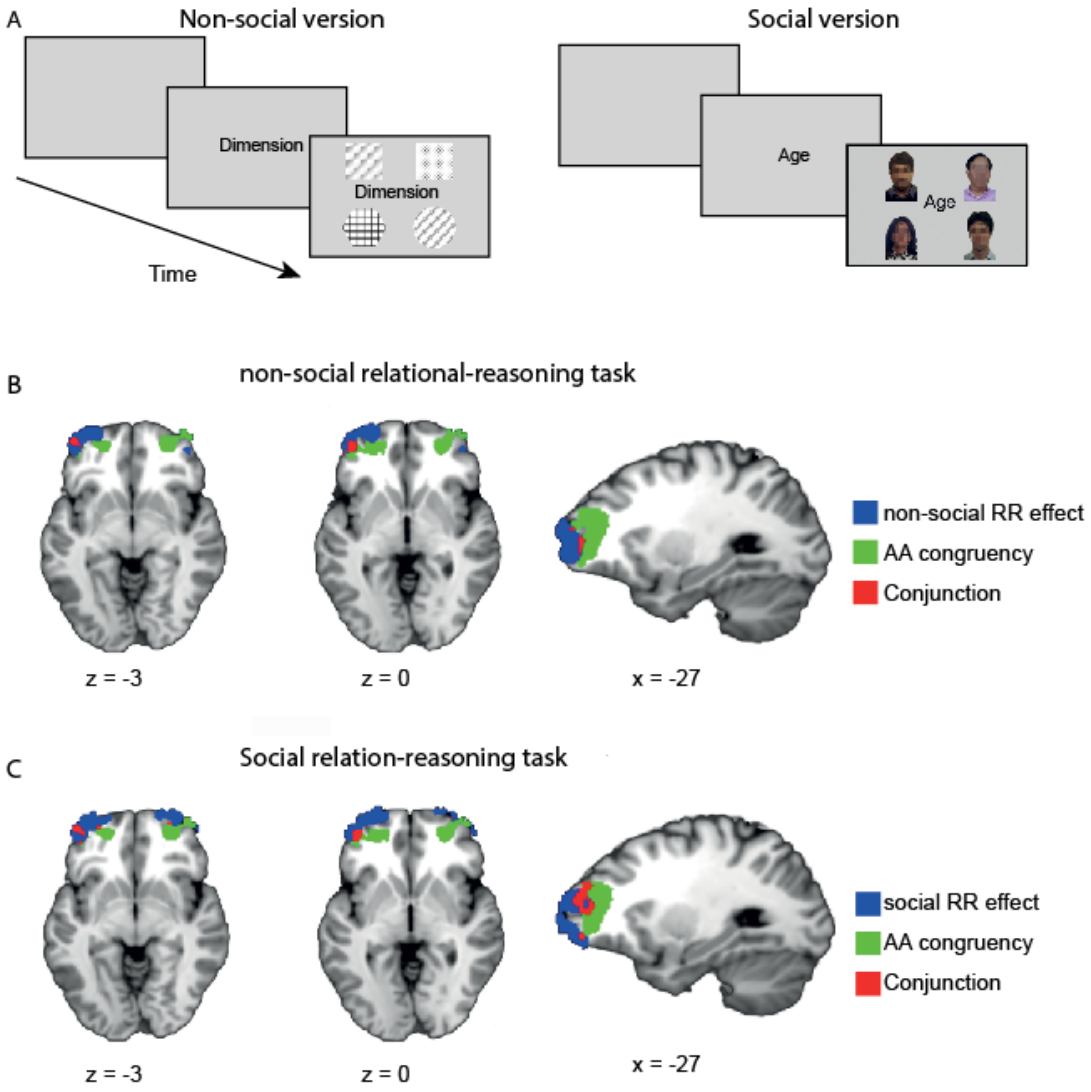

Figure 4: Distinct FPl sub-structures in social-emotional control and higher-order relational reasoning

A) This panel shows both versions of the relational-reasoning task. The non-social panel depicts a high-order trial where participants had to make a judgement about the relation between dimensions (e.g. whether both pairs matched on shape or texture). The social panel depicts a low-dimension trial in which participants had to indicate whether there was a match in age in one or both of the pairs. B) This panel shows the (lack of) conjunction of the congruency effect in the AA task (red); the non-social relational reasoning (RR) effect during the task developed by Vendetti and Bunge (2014) (green); and the conjunction between the two (blue). C) This panel shows the conjunction of the congruency effect

in the AA task (red); the social relational-reasoning effect during the task developed by Hartogsveld et al., (2017) (green); and the conjunction between the two (blue). For both tasks there is some overlap of effects in Area 46, but only a few voxels in FPl. Coloured areas illustrate clusters surviving cluster correction at z > 2.3.

Discussion

The present study anatomically qualifies the involvement of the anterior prefrontal cortex in social-emotional control. There are three main findings. First, structural and functional connectivity fingerprints of the lateral Frontal Pole (Neubert et al. 2014) closely match the fingerprints of the aPFC territory recruited when social-emotional control is required. Second, the strength of FPl structural connectivity with the amygdala accounts for a substantial portion of inter-individual variation in social-emotional regulation abilities. Third, socio-emotional regulation and relational reasoning are supported by contiguous but largely distinct portions of the FPl. These findings provide evidence for a precise cortical region (FPl) and a structural pathway (the ventral amygdalofugal bundle) through which a cognitively complex form of regulation might be implemented in the human brain, while differentiating emotional regulation from the neural implementation of other cognitive processes known to be supported by the FPl (Vendetti and Bunge 2014).

FPl supports social-emotional control

Previous work has repeatedly shown that the aPFC is involved in controlling social-emotional behaviour, and that it is capable of doing so by influencing downstream activity in the amygdala (Volman et al. 2013; Tyborowska et al. 2016); motor cortex; and parietal areas (Volman et al. 2011; Bramson et al. 2018). Here, we extend this knowledge by showing that the aPFC contribution to social-emotional control (e.g. Volman et al. 2011; Tyborowska et al. 2016) arises from a precise anatomical structure: the lateral Frontal Pole (Neubert et al. 2014). This finding is based on the

464 connectivity fingerprint of the FPl. This anatomical metric also provides clues to the information
465 received by the FPl, and the influence it can exert on other brain structures (Mars et al. 2018). The
466 FPl, differently from neighbouring areas FPm and 46, is connected to both medial and lateral circuits
467 with parietal, cingulate, and temporal regions (Figure 2). The peculiar pattern of FPl connectivity fits
468 with the known supramodal regulatory role of this area during social-emotional control (Volman et
469 al. 2011; Volman et al. 2013; Koch et al. in prep), and with the notion that social-emotional
470 regulation involves access to both egocentric value of emotionally-laden actions, as well as social
471 consequences of those actions (Koch et al. 2018).

472 This study was designed to add functional specificity to those anatomically-grounded
473 inferences on FPl contributions to social-emotional regulations, given that the aPFC region has
474 consistently been involved in supporting several cognitive processes, e.g. concurrent monitoring of
475 current and alternative goals (Burgess et al. 2007; Badre and D'esposito 2009; Mansouri et al. 2017),
476 cognitive exploration (Daw et al. 2006; Zajkowski et al. 2017), counterfactual reasoning (Boorman et
477 al. 2009b; Koechlin 2016), metacognition (Fleming et al. 2014; Shekhar and Rahnev 2018), and
478 relational reasoning (Vendetti and Bunge 2014; Hartogsveld et al. 2017). We considered the
479 possibility that the social-emotional regulation operationalized in the approach-avoidance task
480 entails monitoring rule-based relations between emotional stimuli and emotional actions. On that
481 premise, both social-emotional regulation and relational reasoning would involve a re-representation
482 of relations between stimuli. The marginal spatial overlap between the FPl territories supporting the
483 approach-avoidance and relational-reasoning tasks argues against the possibility that those two tasks
484 share a re-representational process. It could be argued that the current finding is a consequence of
485 differences in the content of the material being processed by the FPl in the approach-avoidance and
486 relational-reasoning tasks. However, other studies have shown that, in both tasks, the FPl operates
487 on supramodal representations (Koch et al. in prep; Hartogsveld et al. 2017). Furthermore, the
488 spatial overlap between AA and RR tasks remains marginal even when both tasks used faces as input
489 material (Figure 4C). It remains to be seen whether the FPl contribution to social-emotional control

can be better explained by other cognitive processes associated with this region (Koch et al. 2018), or whether the cognitive demands of social-emotional control and their input-output connectivity segregate this faculty from other known FPl functions.

Amygdala-prefrontal projections modulate control over emotional-action

This study shows that control over social-emotional actions is negatively associated with the strength of amygdala-FPl connections. On the assumption that the amygdala-FPl connectivity indexed in this study captures the amygdalofugal pathway (Folloni et al. 2019), i.e. the main efferent pathways from amygdala to frontal cortex (Krüger et al. 2015; Kamali et al. 2016), the finding suggests that stronger amygdala projections to the FPl impairs emotional regulation. Namely, during incongruent trials, stronger amygdala afferences to the FPl could lead to stronger automatic action tendencies or heightened emotional vigilance and thus more errors when those tendencies need to be rapidly over-ruled. This observation fits with previous imaging work showing that successful emotional control reduces effective bottom-up connectivity between amygdala and aPFC (Volman et al. 2013). This observation also suggests that top-down regulatory FPl efferences might reach the amygdala through other fiber bundles, e.g. the uncinate fasciculus (Petrides and Pandya 2007); or through other regions, e.g. the nucleus accumbens (Wager et al. 2008) or the orbitofrontal cortex (Ray and Zald 2012). Future studies could test for behavioural consequences of this potential anatomical dissociation between bottom-up and top-down amygdala-FPl connectivity, a particularly relevant topic given that most of our knowledge on amygdala-prefrontal connectivity stems from anthropoid monkeys, which do not possess a functional homologue of the human lateral Frontal Pole (Semendeferi et al. 2010; Neubert et al. 2014; Mars et al. 2016).

Interpretational issues

513 It could be argued that regulating social–emotional behaviour is just an instance of inhibitory
514 control, and that it could be accomplished by suppressing automatic emotional action tendencies
515 (Aron et al. 2014). Although previous studies have shown that a simple inhibitory mechanism is not
516 sufficient to explain how individuals select courses of action alternative to their prepotent tendencies
517 (Roelofs et al. 2008; Koch et al. 2018), it remains to be tested whether the involvement of the inferior
518 frontal gyrus observed in this study reflects inhibitory control, or rule selection together with area 46
519 (Rowe et al. 2000).

520 In principle, the relation between strength of amygdala-FPl connectivity and behavioural
521 emotional control could be explained by a third factor, e.g. trait anxiety. However, the tract strength
522 between amygdala and FPl did not correlate with trait anxiety, and the correlation between
523 behavioural congruency and tract strength remained when controlling for anxiety. This observation
524 confirms that, in healthy participants, aPFC activity during the AA task is orthogonal to trait anxiety
525 effects (Bramson et al. 2018), in contrast to known trait anxiety effects on amygdala-vmPFC
526 connectivity (Kim and Whalen 2009).

527 It is not easy to acquire reliable fMRI signals from anterior prefrontal regions (Hutton et al.
528 2002). Therefore, we used magnetic field corrections to restore signal distortions around the frontal
529 pole (Jezzard and Balaban 1995; Jenkinson 2004). The resting-state connectivity profiles closely
530 matched those of earlier studies that used different MRI protocols (Neubert et al. 2014; Mars et al.
531 2016) arguing against the possibility that the results reported here can be attributed to signal
532 distortions.

533 **Conclusion**

534 This study provides anatomical evidence supporting the involvement of the lateral frontal
535 pole in the regulation of social-emotional behaviour (Koch et al. 2018). The findings have implications
536 for structuring mechanism-based interventions in psychopathologies characterized by altered
537 emotional control abilities, e.g. anxiety disorders and psychopathy (Volman et al. 2016). The findings

are also relevant for understanding the neurobiological and cognitive complexities underlying rule-based regulation of action tendencies, arguably a crucial pre-requisite for the development of human cumulative culture (Hare 2017; Whiten 2017).

Funding

This work was supported by a VICI grant (#453-12-001) from the Netherlands Organization for Scientific Research (NWO) and a starting grant from the European Research Council (ERC_StG2012_313749) awarded to Karin Roelofs. The work of RBM is supported by the Netherlands Organization for Scientific Research (NWO) [452-13-015]. The work of DF was supported by Wellcome Trust UK Grant (105238/Z/14/Z).

References

Andersson JLR, Skare S, Ashburner J. 2003. How to correct susceptibility distortions in spin-echo echo-planar images: application to diffusion tensor imaging. Neuroimage. 20:870–888.

Andersson JLR, Sotiropoulos SN. 2016. An integrated approach to correction for off-resonance effects and subject movement in diffusion MR imaging. Neuroimage. 125:1063–1078.

Aron AR, Robbins TW, Poldrack RA. 2014. Inhibition and the right inferior frontal cortex: one decade on. Trends Cogn Sci. 18:177–185.

Badre D, D'esposito M. 2009. Is the rostro-caudal axis of the frontal lobe hierarchical? Nat Rev Neurosci. 10:659–669.

Beckmann CF, Smith SM. 2004. Probabilistic independent component analysis for functional

560 magnetic resonance imaging. IEEE Trans Med Imaging. 23:137–152.

561 Behrens TEJ, Berg HJ, Jbabdi S, Rushworth MFS, Woolrich MW. 2007. Probabilistic diffusion
562 tractography with multiple fibre orientations: What can we gain? Neuroimage. 34:144–155.

563 Boorman ED, Behrens TEJ, Woolrich MW, Rushworth MFS. 2009a. How Green Is the Grass on the
564 Other Side? Frontopolar Cortex and the Evidence in Favor of Alternative Courses of Action.
565 Neuron. 62:733–743.

566 Boorman ED, Behrens TEJ, Woolrich MW, Rushworth MFS. 2009b. How green is the grass on the
567 other side? Frontopolar cortex and the evidence in favor of alternative courses of action.
568 Neuron. 62:733–743.

569 Bramson B, Jensen O, Toni I, Roelofs K. 2018. Cortical oscillatory mechanisms supporting the control
570 of human social-emotional actions. J Neurosci. 3317–3382.

571 Burgess PW, Dumontheil I, Gilbert SJ. 2007. The gateway hypothesis of rostral prefrontal cortex (area
572 10) function. Trends Cogn Sci. 11:290–298.

573 Daw ND, O'doherty JP, Dayan P, Seymour B, Dolan RJ. 2006. Cortical substrates for exploratory
574 decisions in humans. Nature. 441:876–879.

575 Eklund A, Nichols T, Knutsson H. 2015. Can parametric statistical methods be trusted for fMRI based
576 group studies? Proc Natl Acad Sci. 113:7900–7905.

577 Etkin A, Büchel C, Gross JJ. 2015. The neural bases of emotion regulation. Nat Rev Neurosci. 16:693.

578 Fleming SM, Ryu J, Golfinos JG, Blackmon KE. 2014. Domain-specific impairment in metacognitive
579 accuracy following anterior prefrontal lesions. Brain. 137:2811–2822.

580 Folloni D, Sallet J, Khrapichev AA, Sibson NR, Verhagen L, Mars RB. 2019. Two fiber pathways
581 connecting amygdala and prefrontal cortex in humans and monkeys. bioRxiv. 561811.

582 Ghashghaei HT, Barbas H. 2002. Pathways for emotion: interactions of prefrontal and anterior
583 temporal pathways in the amygdala of the rhesus monkey. Neuroscience. 115:1261–1279.

584 Ghashghaei HT, Hilgetag CC, Barbas H. 2007. Sequence of information processing for emotions based
585 on the anatomic dialogue between prefrontal cortex and amygdala. Neuroimage. 34:905–923.

586 Griffanti L, Douaud G, Bijsterbosch J, Evangelisti S, Alfaro-Almagro F, Glasser MF, Duff EP, Fitzgibbon
587 S, Westphal R, Carone D. 2017. Hand classification of fMRI ICA noise components. Neuroimage.
588 154:188–205.

589 Hare B. 2017. Survival of the friendliest: Homo sapiens evolved via selection for prosociality. Annu
590 Rev Psychol. 68:155–186.

591 Hartogsveld B, Bramson B, Vijayakumar S, van Campen AD, Marques JP, Roelofs K, Toni I, Bekkering
592 H, Mars RB. 2017. Lateral frontal pole and relational processing: Activation patterns and
593 connectivity profile. Behav Brain Res.

594 Hutton C, Bork A, Josephs O, Deichmann R, Ashburner J, Turner R. 2002. Image distortion correction
595 in fMRI: a quantitative evaluation. Neuroimage. 16:217–240.

596 Jenkinson M. 2004. Improving the registration of B0-distorted EPI images using calculated cost
597 function weights. In: Tenth International Conference on functional mapping of the human brain.

598 Jenkinson M, Bannister P, Brady M, Smith S. 2002. Improved optimization for the robust and accurate
599 linear registration and motion correction of brain images. Neuroimage. 17:825–841.

600 Jezzard P, Balaban RS. 1995. Correction for geometric distortion in echo planar images from B0 field
601 variations. Magn Reson Med. 34:65–73.

602 Kamali A, Sair HI, Blitz AM, Riascos RF, Mirbagheri S, Keser Z, Hasan KM. 2016. Revealing the ventral
603 amygdalofugal pathway of the human limbic system using high spatial resolution diffusion
604 tensor tractography. Brain Struct Funct. 221:3561–3569.

605 Kim MJ, Whalen PJ. 2009. The structural integrity of an amygdala–prefrontal pathway predicts trait
606 anxiety. J Neurosci. 29:11614–11618.

607 Koch SBJ, Galli A, Volman I, Kaldewaij R, Toni I & Roelofs K. Submitted. Neural control of emotional
608 actions in response to affective vocalizations.

609 Koch SBJ, Mars RB, Toni I, Roelofs K. 2018. Emotional control, reappraised. Neurosci Biobehav Rev.
610 95:528–534.

611 Koechlin E. 2016. Prefrontal executive function and adaptive behavior in complex environments. Curr
612 Opin Neurobiol. 37:1–6.

613 Krüger O, Shiozawa T, Kreifelts B, Scheffler K, Ethofer T. 2015. Three distinct fiber pathways of the
614 bed nucleus of the stria terminalis to the amygdala and prefrontal cortex. Cortex. 66:60–68.

615 Langner R, Leiberg S, Hoffstaedter F, Eickhoff SB. 2018. Towards a human self-regulation system:
616 Common and distinct neural signatures of emotional and behavioural control. Neurosci
617 Biobehav Rev. 90:400–410.

618 Mansouri FA, Koechlin E, Rosa MGP, Buckley MJ. 2017. Managing competing goals-a key role for the
619 frontopolar cortex. Nat Rev Neurosci.

620 Mars RB, Jbabdi S, Sallet J, O'Reilly JX, Croxson PL, Olivier E, Noonan MP, Bergmann C, Mitchell AS,
621 Baxter MG. 2011. Diffusion-weighted imaging tractography-based parcellation of the human
622 parietal cortex and comparison with human and macaque resting-state functional connectivity.
623 J Neurosci. 31:4087–4100.

624 Mars RB, Passingham RE, Jbabdi S. 2018. Connectivity Fingerprints: From Areal Descriptions to
625 Abstract Spaces. Trends Cogn Sci. 22:1026–1037.

626 Mars RB, Verhagen L, Gladwin TE, Neubert F-X, Sallet J, Rushworth MFS. 2016. Comparing brains by
627 matching connectivity profiles. Neurosci Biobehav Rev. 60:90–97.

628 Morawetz C, Bode S, Derntl B, Heekeren HR. 2017. The effect of strategies, goals and stimulus
629 material on the neural mechanisms of emotion regulation: A meta-analysis of fMRI studies.
630 Neurosci Biobehav Rev. 72:111–128.

631 Motzkin JC, Philippi CL, Wolf RC, Baskaya MK, Koenigs M. 2015. Ventromedial prefrontal cortex is
632 critical for the regulation of amygdala activity in humans. Biol Psychiatry. 77:276–284.

633 Neubert F-X, Mars RB, Thomas AG, Sallet J, Rushworth MFS. 2014. Comparison of human ventral
634 frontal cortex areas for cognitive control and language with areas in monkey frontal cortex.
635 Neuron. 81:700–713.

636 Passingham RE, Stephan KE, Kötter R. 2002. The anatomical basis of functional localization in the
637 cortex. Nat Rev Neurosci. 3:606.

638 Petrides M, Pandya DN. 2007. Efferent association pathways from the rostral prefrontal cortex in the
639 macaque monkey. J Neurosci. 27:11573–11586.

640 Ramnani N, Owen AM. 2004. Anterior prefrontal cortex: insights into function from anatomy and
641 neuroimaging. Nat Rev Neurosci. 5.

642 Ray RD, Zald DH. 2012. Anatomical insights into the interaction of emotion and cognition in the
643 prefrontal cortex. Neurosci Biobehav Rev. 36:479–501.

644 Roelofs K, Minelli A, Mars RB, Van Peer J, Toni I. 2008. On the neural control of social emotional
645 behavior. Soc Cogn Affect Neurosci. nsn036.

646 Rowe JB, Toni I, Josephs O, Frackowiak RSJ, Passingham RE. 2000. The prefrontal cortex: response
647 selection or maintenance within working memory? Science (80-). 288:1656–1660.

648 Sallet J, Mars RB, Noonan MP, Neubert F-X, Jbabdi S, O'Reilly JX, Filippini N, Thomas AG, Rushworth
649 MF. 2013. The organization of dorsal frontal cortex in humans and macaques. J Neurosci.
650 33:12255–12274.

651 Semendeferi K, Teffer K, Buxhoeveden DP, Park MS, Bludau S, Amunts K, Travis K, Buckwalter J. 2010.
652 Spatial organization of neurons in the frontal pole sets humans apart from great apes. Cereb
653 cortex. 21:1485–1497.

654 Shekhar M, Rahnev D. 2018. Distinguishing the Roles of Dorsolateral and Anterior PFC in Visual
655 Metacognition. J Neurosci. 38:5078–5087.

656 Tillman RM, Stockbridge MD, Nacewicz BM, Torrisi S, Fox AS, Smith JF, Shackman AJ. 2018. Intrinsic
657 functional connectivity of the central extended amygdala. Hum Brain Mapp. 39:1291–1312.

658 Tyborowska A, Volman I, Smeekens S, Toni I, Roelofs K. 2016. Testosterone during puberty shifts
659 emotional control from pulvinar to anterior prefrontal cortex. J Neurosci. 36:6156–6164.

660 Tzourio-Mazoyer N, Landeau B, Papathanassiou D, Crivello F, Etard O, Delcroix N, Mazoyer B, Joliot
661 M. 2002. Automated anatomical labeling of activations in SPM using a macroscopic anatomical
662 parcellation of the MNI MRI single-subject brain. Neuroimage. 15:273–289.

663 Vendetti MS, Bunge SA. 2014. Evolutionary and Developmental Changes in the Lateral Frontoparietal
664 Network: A Little Goes a Long Way for Higher-Level Cognition. Neuron. 84:906–917.

665 Volman I, Roelofs K, Koch S, Verhagen L, Toni I. 2011. Anterior prefrontal cortex inhibition impairs
666 control over social emotional actions. Curr Biol. 21:1766–1770.

667 Volman I, Toni I, Verhagen L, Roelofs K. 2011. Endogenous testosterone modulates prefrontal–
668 amygdala connectivity during social emotional behavior. Cereb Cortex. bhr001.

669 Volman I, Verhagen L, den Ouden HEM, Fernández G, Rijpkema M, Franke B, Toni I, Roelofs K. 2013.
670 Reduced serotonin transporter availability decreases prefrontal control of the amygdala. J
671 Neurosci. 33:8974–8979.

672 Volman I, von Borries AKL, Bulten BH, Verkes RJ, Toni I, Roelofs K. 2016. Testosterone modulates
673 altered prefrontal control of emotional actions in psychopathic offenders. ENeuro. 3:ENEURO-

674 0107.

675 Wager TD, Davidson ML, Hughes BL, Lindquist MA, Ochsner KN. 2008. Prefrontal-subcortical
676 pathways mediating successful emotion regulation. Neuron. 59:1037–1050.

677 Whiten A. 2017. Culture extends the scope of evolutionary biology in the great apes. Proc Natl Acad
678 Sci. 114:7790–7797.

679 Zajkowski WK, Kossut M, Wilson RC. 2017. A causal role for right frontopolar cortex in directed, but
680 not random, exploration. Elife. 6.

681